

# *A novel flow-guide device for uniform exhaust in a central air exhaust ventilation system*

Article

Accepted Version

Creative Commons: Attribution-Noncommercial-No Derivative Works 4.0

Tong, L., Gao, J., Luo, Z. ORCID: <https://orcid.org/0000-0002-2082-3958>, Wu, L., Zeng, L., Liu, G. and Wang, Y. (2019) A novel flow-guide device for uniform exhaust in a central air exhaust ventilation system. *Building and Environment*, 149. pp. 134-145. ISSN 0360-1323 doi: 10.1016/j.buildenv.2018.12.007 Available at <https://centaur.reading.ac.uk/80997/>

It is advisable to refer to the publisher's version if you intend to cite from the work. See [Guidance on citing](#).

To link to this article DOI: <http://dx.doi.org/10.1016/j.buildenv.2018.12.007>

Publisher: Elsevier

All outputs in CentAUR are protected by Intellectual Property Rights law, including copyright law. Copyright and IPR is retained by the creators or other copyright holders. Terms and conditions for use of this material are defined in the [End User Agreement](#).

[www.reading.ac.uk/centaur](http://www.reading.ac.uk/centaur)

**CentAUR**

Central Archive at the University of Reading

Reading's research outputs online

# A novel flow-guide device for uniform exhaust in a central air exhaust ventilation system

Leqi Tong<sup>1</sup>, Jun Gao\*<sup>1</sup>, Zhiwen Luo<sup>2</sup>, Li Wu<sup>1</sup>, Lingjie Zeng<sup>1</sup>, Guodong Liu<sup>1</sup>, Yirui Wang<sup>1</sup>  
(<sup>1</sup>*Institute of HVAC Engineering, School of Mechanical Engineering, Tongji University, Shanghai 200092, China;* <sup>2</sup>*School of the Built Environment, University of Reading, Reading, UK*)

\*corresponding author, J Gao, Dr., Prof., [gaojun-hvac@tongji.edu.cn](mailto:gaojun-hvac@tongji.edu.cn)

**Abstract:** Exhaust ventilation system with one central fan and multiple terminals has been widely used for the heat and contaminant removal in building environment. Conventional design without pressure balancing leads to uneven distribution of exhaust airflow rate among the multiple outlets. Existed balancing methods usually uses dampers (constant-air-volume valve or regulating valve), tapered duct, or varied inlet area. However, these methods result in higher fan energy consumption, or complicated construction and on-site commissioning. In this paper, a flow-guide device was developed for adjusting the pressure distribution of duct branches. This new device is integrated with the interflow Tee-junction and does not need any commissioning or regulating. The resistance performance of the device responding to the structural parameter was derived using the CFD simulation and experiment. The negative direct resistance featured by the device was found to effectively benefit exhaust at the outlets farther away from the central fan. The ductwork hydraulic model based on the Bernoulli's law of airflow and the fitted resistance correlations were further proposed to fulfill the parametric design. Finally, full-scale test was carried out for a central exhaust system installed with the flow-guide devices referring to a factory workshop with 30 heat and contaminant sources. Compared to the system without the devices, the total rate of the system increased by 25%. Discrepancy of exhaust rate decreased by 78% and uneven degree decreased by 82%, which well meets the engineering balancing requirement. Meanwhile, total resistance of the system reduced 23.8% owing to the negative loss the devices bring.

**Keywords:** Central exhaust system; Ventilation; Flow guide; Uniform exhaust; Resistance coefficient; Pressure distribution

## Nomenclature

$P$	Static pressure (Pa)
$E$	Energy Consumption of the central fan (kW)
$v$	Velocity (m/s)
$P_t$	Pressure head of the terminal fan (Pa)
$\Delta P_{sys}$	Total pressure loss of the system (Pa)
$Q$	Airflow rate (m <sup>3</sup> /h)
$L$	Distance between the adjacent exhaust terminals (mm)
$n$	Number of exhaust terminal hoods

1	$A$	Cross Sectional Area ( $m^2$ )
2	$Re$	Reynold Number
3	$K$	Roughness degree of main duct (mm)
4	$a,b,c,d,e$	Constants in regression formulas
5	$D_e$	Hydraulic diameter of main duct (m)
6	Greek Symbols	
7	$g$	Gravity acceleration ( $m^2/s$ )
8	$\rho$	Density ( $kg/m^3$ )
9	$\xi_{dir}, \xi_{con}$	Direct and confluent resistance coefficient
10	$\xi$	Frictional resistance coefficient
11	$\xi_c$	Resistance coefficient of the elbow in branch#1
12	$\beta$	Exhaust uneven degree of the system
13	Subscripts	
14	$i$	Calculation node number
15	m	Main duct
16	b	Branch duct
17	d	Design Value
18	$fc$	Front position along flow direction in main duct
19	$bc$	Back position along flow direction in main duct
20	$ave,max,min$	Average, maximum and minimum of all terminals

21

## 22 **1 Introduction**

23 The air exhaust ventilation system with one central fan and multiple terminals has been  
 24 widely used for heat and contaminant removal in various types of buildings, i.e., heat extraction  
 25 for train braking in subway station [1], exhaust ventilation in Chinese restaurant with multiple  
 26 dining rooms, pollutant removal in an industrial workshop with multiple sources [2, 3] and so on.  
 27 For those applications, pressure balancing is always required to ensure a sufficient and uniform  
 28 exhaust ventilation.

29 The air system balancing is related with duct sizing [4] in design period, and testing,  
 30 adjusting and balancing (TAB) after installation is completed [5]. Traditional duct design methods  
 31 for air systems include Equal friction method, Static regain method and the T-method.  
 32 Equal-friction method keeps the designed ducts possessing a constant total pressure loss per unit  
 33 loss [6], which is sometimes hard to achieve in real world design. Static regain method changes  
 34 downstream duct sizes to obtain the same static pressure at diverging flow junctions [7], which is  
 35 only applicable for supply air system. These two methods are both non-optimizing methods, while  
 36 the T-method is a practical optimization method with dynamic programming procedure [8].  
 37 T-method pursues both pressure equilibrium and the least life-cycle cost, which is well applied in  
 38 some factory exhaust systems[9]. Tapered central duct or varied branch duct can be adopted in

1 these exhaust systems [10-12] to adjust the major losses by differing the size of each duct section.  
2 Theoretically, self-balancing can be achieved using this kind of method. However, it requires  
3 complicated construction and the extra needed reduction couplings used to joint ducts with various  
4 sizes as well as the tapered duct itself could contribute to the total system resistance. Thus,  
5 uniform cross-sectional ducts are still widely applied and balancing dampers (commonly  
6 regulating valve) are necessary in these systems. Even though the self-balancing design method  
7 has been taken, dampers are still suggested due to the accuracy limitations. Therefore, except for  
8 duct sizing, regular TAB process is always required to regulate flow rates to match load  
9 requirements over full operating ranges. The most difficulty is the complex interaction between  
10 terminals[13]. Traditional methods for dampers' adjustment are commonly target method [14, 15],  
11 which are inaccurate and time-consuming due to their inefficient trail-and-error nature in the  
12 manually regulating procedure. The outcomes largely depend on engineers' experience. To  
13 overcome this problem, simplified way by using the ratio of the junction pressure (SPJ') to the  
14 hood static pressure (SPH') for each branch was proposed to avoid repeated velocity  
15 determinations that required before [16].Some new methods based on both theoretical calculation  
16 model and measuring feedback data have been also studied and made some improvements [17-20].  
17 While the on-site commissioning process is still complex and costs much time and labor power  
18 especially when the number of terminal branches is excessively high. To prevent this troublesome  
19 process, some kinds of automatic regulating dampers like constant-air-volume valve is sometimes  
20 highly abused. Although they that can automatically adjust the airflow rate to the set value as  
21 pressure changes, they bring much more flow resistance and give rise to a largely higher fan  
22 energy consumption.

23 The fan energy consumption caused by the flow resistance of ventilation and air-conditioning  
24 systems is approximately 15%-30% of the total energy consumption in some public buildings of  
25 China. [21, 22]. Many scholars have devoted to the research on resistance reduction in central air  
26 system. Tee-junction can be commonly found in duct systems and their significant resistance  
27 effect has drawn lots of attention. Gan et al[23] founded that the junction pressure-loss coefficient  
28 is dependent on the flow ratio through CFD method. For combining flows, the coefficient for a leg  
29 increases with the proportion of flow it contributes to the total flow. In some occasions, the  
30 phenomenon of negative "loss" coefficients occurred for turbulent branched flows through the  
31 combining junctions. Bastian et al[24] investigated this phenomenon systematically and suggested  
32 it was due to the mutual energy transfer between the two partial flows. Li et al [25] founded that  
33 the eddy and velocity shock existed in the corner of the T-junction and Y-junction leading to great  
34 resistance. A kind of arc-junction was designed and it presented that the eddy disappeared and the  
35 maximum of velocity peak declined in it. They found the arc-junction could show the lowest loss  
36 with proper curvature radius. Gao et al proposed a kind of protrusion structure[26] based on  
37 biomimicry of the branched structure of plants and furtherly made some optimization on the  
38 structure [27], resulting that the reduction rate of the local resistance in a duct tee could be as

1 much as 36% and 21% in two flow directions. By adding the guide vane in the proper position of  
2 the dividing flow tee, Gao et al [28] found that the resistance reduction rate reached 4.3%–263.8%  
3 under different flow ratios and different aspect ratios. Yin et al [29] experimentally found the flow  
4 loss of Tee-junction with the guide vanes at different angles in the branch duct. Haskew et al [30]  
5 studied the effect of the guide vane on an 80° elbow of a circular duct, showing that the vaned  
6 bend under reasonable setting effectively provides uniform stream, reduces cross-stream velocities,  
7 and significantly reduces total pressure losses. Sun et al [31] proposed an optimal position where  
8 the guide plates should be set in the 90° elbow of the circular duct by numerical simulation.  
9 Besides, researches on the flowing characteristics of other flow components and the optimization  
10 for resistance reduction have been also found in [32-35]. However, the loss reduction of the  
11 balancing components in central ventilation system (like constant-air-volume valve) have been  
12 less studied. Existed automatic balancing dampers still result in high fan energy consumption.  
13 Therefore, it is significant to invent a kind of balancing device with simple construction that does  
14 not need regulation or commission after design, which can replace the normal balancing dampers  
15 and do not bring extra resistance or even reduce resistance in the system. The aim of this article is  
16 to investigate the performance of the flow-guide device we developed. Both the resistance  
17 characteristic of the device and its usage in the central air exhaust system were studied. Its  
18 outstanding performance for the uniform exhaust and resistance reduction were discovered and  
19 discussed, which showed its advantages over the normal balancing devices.

## 20 21 ***2 A novel T-junction with a flow-guide structure***

22 This paper proposed a novel flow-guide device that is integrated into the Tee-junction with  
23 low resistance for the balancing of central exhaust system. **Fig1** shows the overall research  
24 structure of this paper. Firstly, a novel flow-guide device was proposed. Both experiment and  
25 numerical simulation were undertaken to understand the resistance characteristics of the device  
26 with different structural parameters under diverse flow ratios. Parametric design method for  
27 exhaust ventilation system installed with the devices was then proposed, combining with the fitted  
28 resistance relations of the device and the ductwork hydraulic model. Finally, the devices were  
29 applied in a real exhaust ventilation system which served for a workshop with 30 heat and  
30 pollutant sources in Shanghai. Full-scale test was carried out to validate the performance of the  
31 devices. Comparison of the total pressure loss of the system between the device and the ideal  
32 regulating valve was further discussed. The influence of major losses, which is due to friction  
33 between the airflow and internal surface of the main duct, and terminal number upon the  
34 flow-guide device system were also studied.

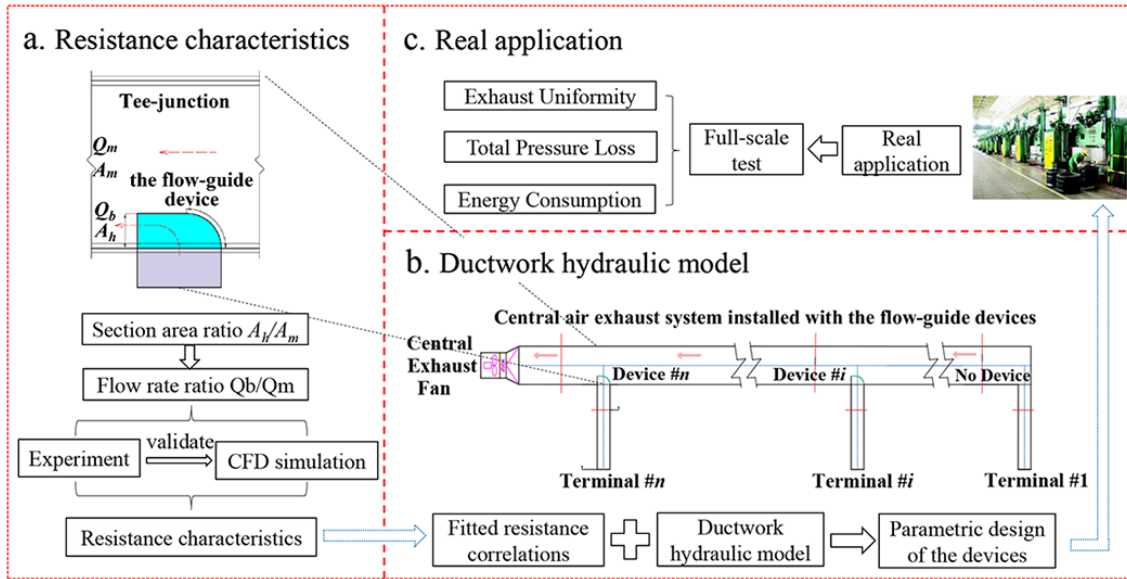


**Fig.1** Overall research structure of this paper

### 2.1 Development of a flow-guide structure

The resistance characteristics of interflow junctions has been already widely discussed. The total pressure loss due to the combining flow mainly results from flow separation at sharp edges [36] and subsequent irreversible airflow collision in the mixing process [37], as is shown in **Fig.2 (a,b)**. While the branch flow and the main flow cross each other perpendicularly in T- or in Y-junction, the resultant airflow collision could cause intensive turbulence and great flow resistance along the main duct. In order to prevent this situation, a partial-arc structure is added at the outlet of the branch that “guides” the branch flow into the main flow without distinct collision, as shown in **Fig.2(c)**. In this occasion, the branch flow direction ideally turns parallel to the main, which could decrease the flow collision and turbulence generation to some extent, thus achieving lower total pressure losses. Such paralleled effect reduced significantly the mutual momentum loss when the main and branch flows merged at the junction.

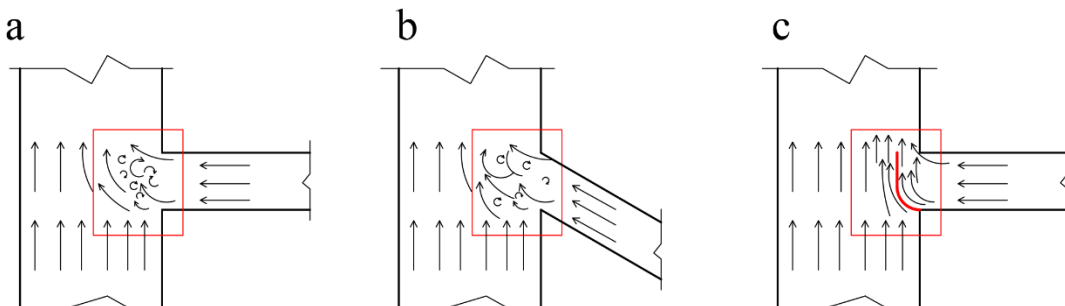
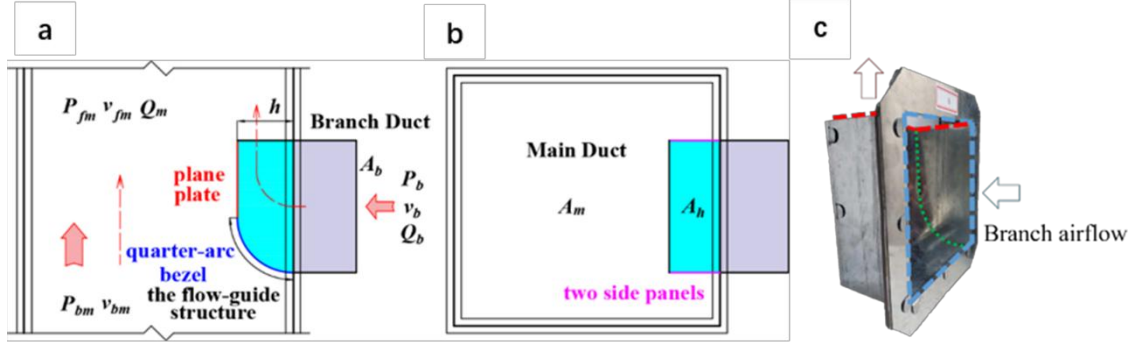


**Fig.2** Flow collision in the junctions: **(a)** Intensive flow collision in 90° Tee; **(b)** Reduced flow collision in Y-junction; **(c)** Ideally Paralleled flow converging through flow guider

To achieve ideally paralleled combining of the main and branch flows in the junction, we

1 developed a flow-guide structure and added it in the junction as shown in **Fig.3**. The structure  
 2 consists of two side panels and a quarter-arc bezel with a consecutive plane plate. The three parts  
 3 encloses a flow region connecting the inflow from the branch and the outflow to the main duct.  
 4 **Fig.3** showed the schematic of the flow-guide device and its installation in Tee as well as the real  
 5 manufactured device.

6



7 **Fig.3** Schematic of the flow-guide device and its installation in the T-junction: (a) Side view along  
 8 the main flow direction (b) Sectional view at the main duct (c) The manufactured device

9

## 10 2.2 Definition of resistance coefficients

11 Given that there are different flow directions in the Tee-junction, there come with two  
 12 different resistance coefficients, namely confluent and direct resistance coefficients, which are two  
 13 vital parameters to describe its characteristics. The direct resistance coefficient presents the total  
 14 pressure loss along the main flow direction and the confluent resistance coefficient reflects the  
 15 total pressure loss along the branch flow direction in combining flow. They are defined as follows:

16

$$17 \quad \xi_{dir} = \frac{\left(P_{fm} + \frac{\rho v_{fm}^2}{2}\right) - \left(P_{bm} + \frac{\rho v_{bm}^2}{2}\right)}{\frac{\rho v_{fm}^2}{2}} \quad (1)$$

$$18 \quad \xi_{con} = \frac{\left(P_{fm} + \frac{\rho v_{fm}^2}{2}\right) - \left(P_b + \frac{\rho v_b^2}{2}\right)}{\frac{\rho v_{fm}^2}{2}} \quad (2)$$

19 Where the  $P_{fm}$ ,  $P_{bm}$  are the static pressure of the front and back position along the flow direction in  
 20 the main duct;  $v_{fm}$ ,  $v_{bm}$  are the velocity of the front and back position along the flow direction in  
 21 the main duct;  $P_b$  and  $v_b$  are the static pressure and velocity of the branch position. More details  
 22 are shown in Fig.4.

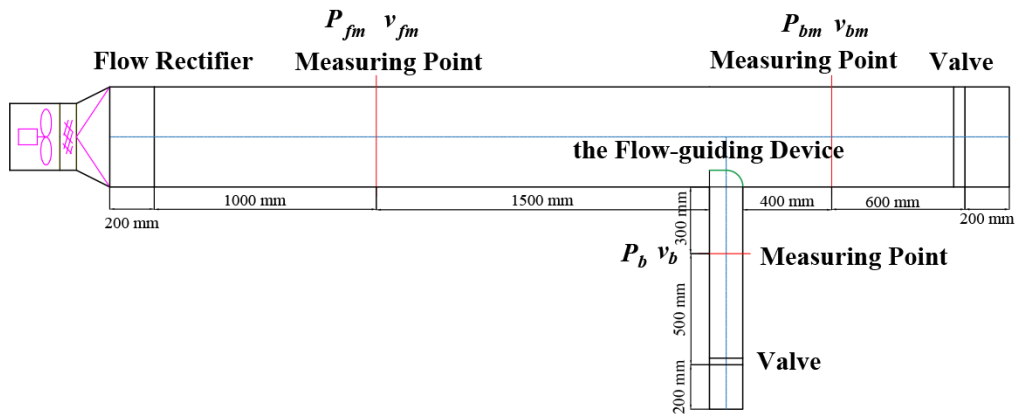
23 The resistance coefficients have been found related to two parameters of the traditional  
 24 T-junction, i.e., the confluent ratio of flow rate  $Q_b/Q_m$  and the sectional area ratio  $A_b/A_m$ . Blaisdell  
 25 and Manson[38] proposed quadratic functional equations to correlate the resistance coefficients of  
 26  $90^\circ$  T-junction to these two parameters. Other researchers [39-41] also proved that the resistance  
 27 coefficients of the  $90^\circ$  T-junction are determined by the two ratios. Compared to a traditional  $90^\circ$

1 T-junction, a structural parameter, the depth the device stretched into the main duct  $h$ , was  
 2 introduced in the flow-guide device. This depth represents the momentum proportion in the  
 3 combing flows and it is functioned as adjusting the cross-section area of the branch outlet. It  
 4 means this structural parameter still indicates the effect of the sectional area ratio. In this new  
 5 device, however, the sectional area ratio should be defined as  $A_h/A_m$ . The resistance characteristics  
 6 of the device were therefore defined under the flow rate ratio  $Q_b/Q_m$  and the sectional area ratio  
 7  $A_h/A_m$ .

8

9 *2.3 Experiment and CFD simulation for resistance coefficients*

10 To achieve the resistance characteristics of the flow-guide device, an experiment setup was  
 11 established as shown in **Fig4**. The main duct was built with a cross-section of 450mmX550mm  
 12 and the branch duct 150mmX150mm. Two valves were installed in both main and branch ducts to  
 13 adjust the flow rate ratio ranging from 0.03 to 0.5. A flow rectifier was used to even the airflow in  
 14 the main duct for the purpose of stabilizing measuring condition. The rated airflow and pressure  
 15 head of the centrifugal exhaust fan are 4500 m<sup>3</sup>/h and 300 Pa, respectively. The flow-guide device  
 16 with five different depth  $h$  as 55mm, 75mm, 95mm, 115mm, and 135mm were applied in the  
 17 experiment, as well as the Tee-junction without the device. Three measuring points were chosen in  
 18 the ducts, one upstream of the device, one downstream and one in the branch. Standard Pitot tube  
 19 and electronic micro-manometer were used to measure the dynamic and static pressure. The  
 20 measurements were repeated three times to ensure the accuracy. The resistance coefficients are  
 21 calculated by Eqs. (1) and (2).



22

23 **Fig.4** Schematic diagram of experiment for the resistance coefficients of flow-guide devices

24

25 Apart from the experiment, the computational fluid dynamics (CFD) simulation was also  
 26 adopted to investigate the resistance characteristics of the flow-guide devices. The effects of  
 27 turbulence models, difference differencing schemes and meshing arrangements on the accuracy of

1 the simulation were studied previously [42]. The standard k- $\epsilon$  turbulence model combined with  
2 the QUICK difference scheme and SIMPLE algorithm for coupling pressure and velocity were  
3 found to be adequate and hence used for the present work. The pressure based segregated solver  
4 and unstructured mesh were chosen.

5 The size of the main and branch ducts was chosen the same as the experiment. The inlets of  
6 main and branch ducts were set as velocity inlet and the set values of velocity were calculated with  
7 different flow ratios according to the experiment. The main duct outlet was set as pressure outlet  
8 and the relative pressure gauge is set as 0 Pa. The device with ten different depths  $h$ , 55 mm ~ 155  
9 mm with increasing rate 10 mm, were simulated. To investigate the overall influence of the  
10 sectional area ratio  $A_m/A_h$  on the resistance characteristics, different cross section of the main duct  
11 was considered in the CFD simulation, while the branch duct keeps as 150\*150 mm and the  
12 structural parameter  $h = 85$  mm.

#### 13 *2.4 Results of resistance coefficients*

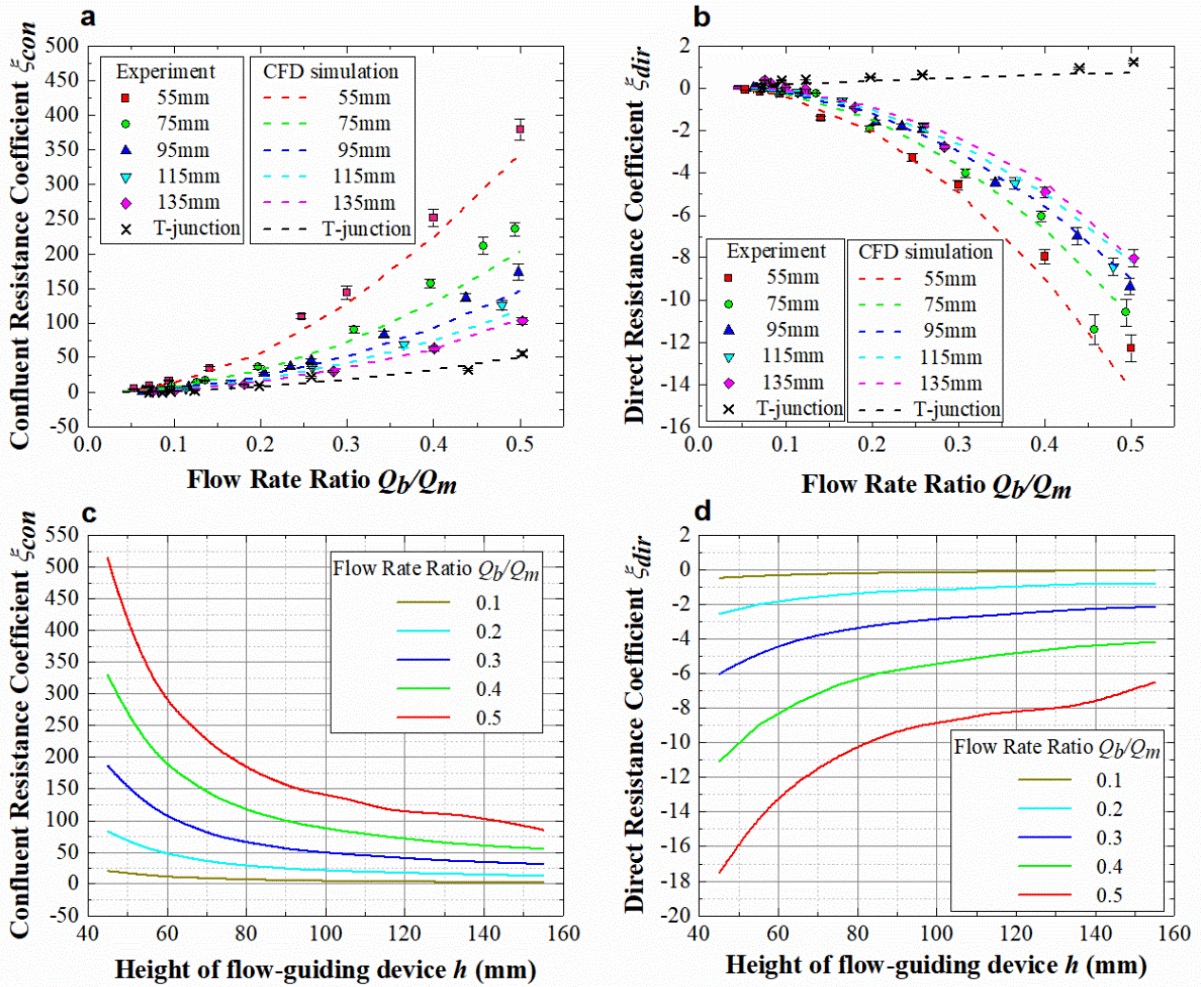
14 As is shown in **Fig.5 (a,b)**, the simulation results agree well with the experiment data. It can  
15 be seen that the resistance characteristics changes with the flow rate ratio  $Q_b/Q_m$  and the sectional  
16 area ratio  $A_h/A_m$ . The confluent resistance coefficient of the device is generally larger than that of  
17 normal Tee, especially in the range of small  $A_h/A_m$  and large  $Q_b/Q_m$ . It is expected that the branch  
18 resistance of the terminals close to the central fan is to be increased with smaller  $A_h/A_m$  to balance  
19 the resistance with the branches far away from the fan, and thus to help even the flow rate among  
20 all the branches. Significant low  $Q_b/Q_m$  occurs at the branches close the fan, the confluence  
21 resistance coefficient there will be not extremely high. In this instance, the new flow-guide device  
22 can act as a regulating valve through adjusting the structural parameter  $h$ .

23 It is exciting that the direct resistance coefficient shows negative values under most range of  
24 different flow rate ratios, being totally opposite to the normal T-junction (see **Fig. 5b**). It is  
25 resulted from the high-velocity airflow being injected into the main duct, as the device narrows  
26 down the branch flow outlet. It can “introduce” the airflow of the main duct and present more  
27 significant effect when the flow rate ratio is high or the size of the device outlet is small. **Fig.6**  
28 presents the velocity distribution of the flow converging area near the flow-guide device.  
29 Turbulent airflow generates while the mainstream and the flow through flow guider converges,  
30 which causes that these two streams are not strictly parallel especially when the height of the  
31 device  $h$  or the flow rate ratio  $Q_b/Q_m$  is higher (see **Fig.6d**). At the outlet of the flow guider, it is  
32 observed that there exists a relatively high-velocity area. The velocity gradient gives rise to the  
33 shear flow pattern at the branch outlet. At the same time, the viscous effect in the airflow leads to  
34 the momentum transfer from the branch flow to the main flow, and thus produce the induction  
35 effect on the main flow, i.e., the negative direct resistance. Such finding is very useful for  
36 balancing flow resistance between the branches close to the fan and those far away from the fan,  
37 and thus even the flow rate among the branches. As mentioned above that the device with lower  
38 depth  $h$  used for the branches close to the fan can only increase the local confluent resistance, but

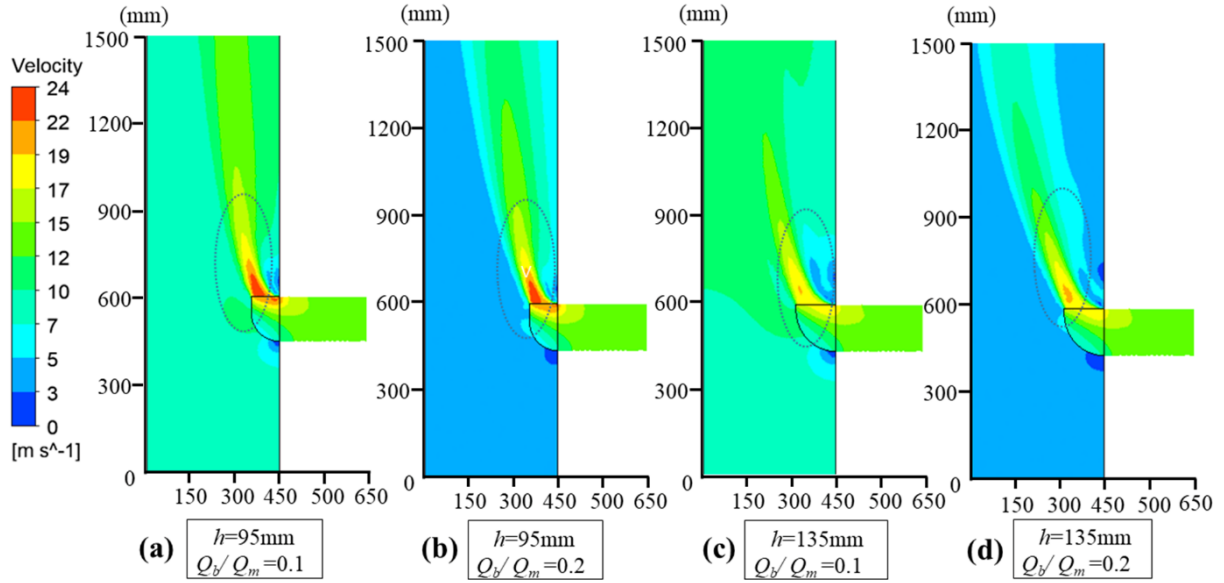
1 merely increase the total resistance for those far away from the fan. While the induction effect  
 2 observed in this work, i.e., the negative direct resistance, help increase the driven force for the  
 3 exhaust flow through far branches. In this situation, the new flow-guide device acts as some  
 4 virtual booster fan in the main duct.

5 To further examine the relationship between the resistance coefficient and the sectional area  
 6 ratio  $A_h/A_m$ , we extend different  $h$  to different sectional area in the CFD simulation. **Fig.7** shows  
 7 that the confluent resistance coefficient increases with the increment of  $Q_b/Q_m$  and decrease with  
 8 increment of  $A_h/A_m$ . It also presents that the direct resistance coefficient decreases with the  
 9 increment of  $Q_b/Q_m$  and increase with increment of  $A_h/A_m$ . It is confirmed that the variation of the  
 10 resistance of the new flow-guide device is determined by the two ratios, similar to the T-junction.

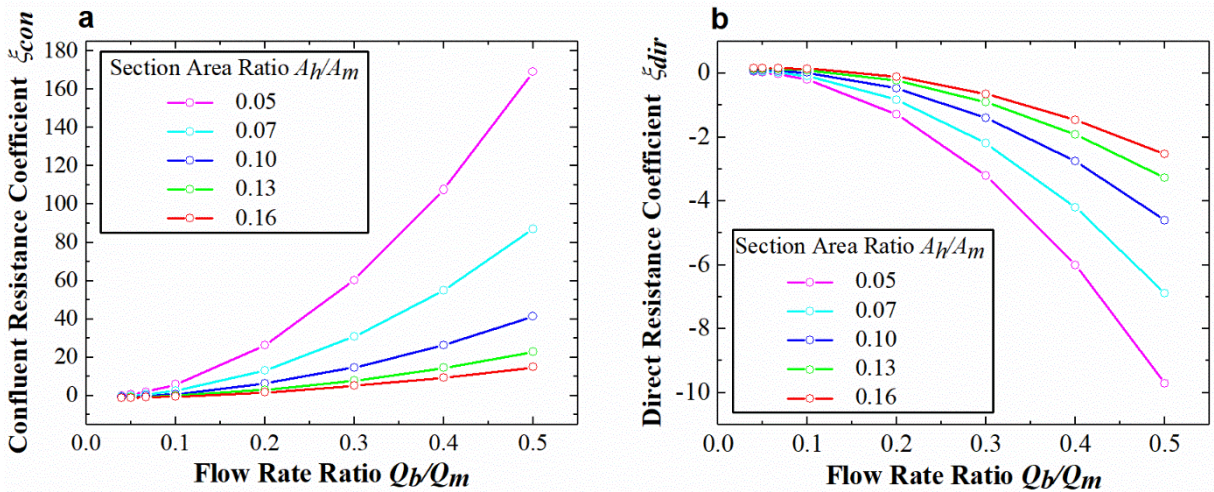
11



12 **Fig.5** Resistance coefficients results: (a) Confluent resistance coefficient curve of the flow-guide  
 13 device with different height under diverse flow rate ratio, comparing the experimental data with  
 14 CFD simulation results; (b) Direct resistance coefficient curve of the device with different height  
 15 and flow rate ratio; (c) Influence of the device height on the Confluent resistance coefficient; (d)  
 16 Influence of the device height on the Direct resistance coefficient



1 **Fig.6** Velocity distribution of the flow converging area near the flow-guide device.



2 **Fig.7** Influence of the section area ratio  $A_h/A_m$  and flow rate ratio  $Q_b/Q_m$  on the resistance  
 3 coefficients of the flow-guide device: (a) Confluent resistance coefficient (b) Direct resistance  
 4 coefficient

5  
 6 Surprisingly, we found that the velocity ratio of the main duct and device outlet  $V_m/V_h$  is the  
 7 key parameter to determine the positive or negative sign of the direct resistance coefficient. The  
 8 critical condition is that  $V_m/V_h=1$ . While the ratio is below one, i.e. the airflow injected from the  
 9 device outlet to the main duct is much faster, it can “introduce” the main flow and lead to negative  
 10 loss. The negative loss effect become much stronger with the velocity ratio decreasing from the  
 11 critical value, for example the flow ratio  $Q_b/Q_m$  increases or the section area ratio  $A_h/A_m$  decreases,  
 12 (see Eq.3). Oppositely, the direct resistance shows positive sign and the flow-guide device would  
 13 add the total pressure loss along the main duct. Therefore, in the design period, it is beneficial to  
 14 make the  $V_m/V_h$  below one as much as possible.

1 
$$\frac{V_m}{V_h} = \left(\frac{A_h}{A_m}\right) / \left(\frac{Q_b}{Q_m}\right) \quad (3)$$

2 Power functional fitting curve was found proper to describe the correlation between the ratio  
 3 of direct resistance coefficient to flow rate ratio  $\xi_{dir}/(Q_b/Q_m)$  and the velocity ratio  $V_m/V_h$   
 4 (see, **Eq.4**). Confluent resistance coefficient  $\xi_{con}$  is found second-order parabolic correlated with  
 5 the ratio of direct resistance coefficient to flow rate ratio  $\xi_{dir}/(Q_b/Q_m)$  (see **Eq.5**). The fitted data  
 6 contains all kinds of combination of the two ratios  $Q_b/Q_m$  and  $A_h/A_m$  we studied in this paper.

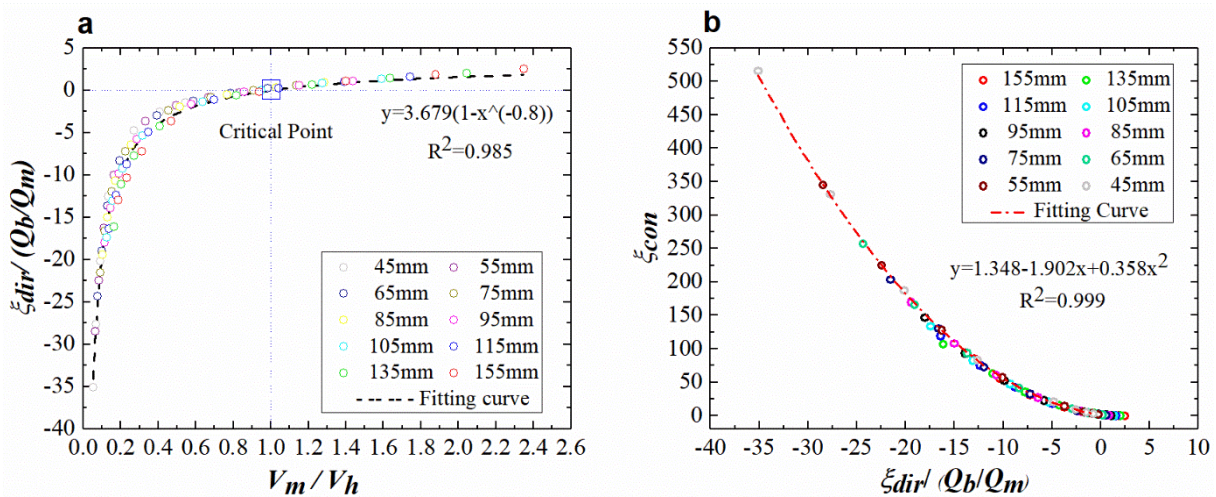
7 
$$\xi_{dir}/\left(\frac{Q_b}{Q_m}\right) = a\left[1 - \left(\frac{V_h}{V_m}\right)^{-b}\right] \quad (4)$$

8 Where  $a=3.679$ ;  $b=0.8$ ,  $Q_b/Q_m$  is in the range of 0.03-0.5 and  $A_h/A_m$  is in the range of 0.03-0.1.

9 
$$\xi_{con} = c[\xi_{dir}/\left(\frac{Q_b}{Q_m}\right)]^2 + d[\xi_{dir}/\left(\frac{Q_b}{Q_m}\right)] + e \quad (5)$$

10 Where  $c=0.358$ ,  $d=-1.902$ ,  $e=1.348$ ,  $Q_b/Q_m$  is in the range of 0.03-0.5.

11 **Fig.8** depicts the power functional and the parabolic correlations discussed above,  
 12 respectively, which clearly reflects the overall resistance characteristics of the new flow-guide  
 13 device. By using these correlations, it becomes possible to assign suitable branch outlet size  $h$   
 14 for each exhaust terminal to achieve even flow rate without a regulating or constant-air-volume valve,  
 15 which usually have significantly high maximum total pressure loss and lead to high fan-power  
 16 consumption of exhaust ventilation system.



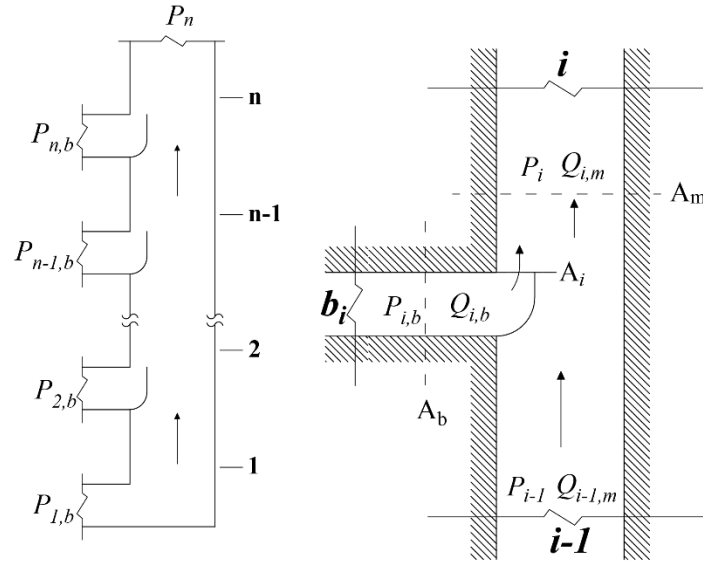
17 **Fig.8** Relationships between the resistance coefficients of the flow-guide device: (a) Power  
 18 functional relationship between the ratio of direct resistance coefficient to flow rate ratio  $\xi$   
 19  $_{dir}/(Q_b/Q_m)$  and the velocity ratio of  $V_m/V_h$  (b) Second-order parabolic relationship between the  
 20 confluent resistance coefficient  $\xi_{con}$  and the ratio of direct resistance coefficient to flow rate ratio  
 21  $\xi_{dir}/(Q_b/Q_m)$ .

1  
2  
3  
4  
5  
6  
7  
8  
9

### 3 Ductwork hydraulic model for central exhaust system

#### 3.1 Mathematical model for ductwork flow

To assign reasonable value of structural parameter of the device among multiple terminals to achieve uniform exhaust, we further extend the work built in **Sec.2** with only one branch duct into a central exhaust system with  $n$  terminals (See **Fig.9**). A ductwork hydraulic model was built up based on the Bernoulli's law and airflow continuity.



10 **Fig.9** Central exhaust system with  $n$  terminals and the calculation node  $i$  of the system

11  
12  
13

According to the Bernoulli's law, we can establish two equations of energy conservation for the airflow from  $i-1$  to  $i$  and from  $b_i$  to  $i$  as follows

14 
$$(P_{i-1} + \frac{\rho Q_{i-1,m}^2}{2A_m^2}) - (P_i + \frac{\rho Q_{i,m}^2}{2A_m^2}) = \frac{\rho Q_{i,m}^2}{2A_m^2} (\xi_i + \xi_{dir,i}) \quad (6)$$

15 
$$(P_{i,b} + \frac{\rho Q_{i,b}^2}{2A_{b,i}^2}) - (P_i + \frac{\rho Q_{i,m}^2}{2A_m^2}) = \frac{\rho Q_{i,m}^2}{2A_m^2} \xi_{con,i} + \frac{\rho Q_{i,b}^2}{2A_{b,i}^2} \xi_{b,i} \quad (7)$$

16 Where  $P_{i,b}$  is static pressure of the branch inlet, regarded as the atmospheric pressure of the  
17 environment;  $\xi_{b,i}$  is the total resistance coefficient at the branch  $b_i$ ;  $\xi_i$  denotes the major loss of  
18 the main duct between  $i-1$  and  $i$ , which is caused by the friction between airflow and internal duct  
19 surface and is calculated by [43]

20 
$$\xi_i = 0.11 \left( \frac{K}{D_e} + \frac{68}{Re_i} \right)^{0.25} \left( \frac{L}{D_e} \right) \quad (8)$$

1 where  $Re$  is Renold Number.  $L$  is length between the adjacent branches.  $K$  is roughness degree of  
 2 internal duct surface.  $De$  is hydraulic diameter of the main duct.

3 To solve Eqs. 6 and 7, we need to take into consideration the equation of mass conservation, i.e.

$$4 \quad Q_{i,m} = iQ_{i,b} = Q_{i-1,m} + Q_{i,b} \quad (9)$$

5 Where the exhaust airflow rate for each branch is constantly  $Q_{i,b}$  due to the uniform exhaust  
 6 pattern concerned in this work.

### 7 3.2 Parametric design of flow-guide devices in the ductwork

8 According to the ductwork hydraulic model presented in Sec. 3.1, the local losses,  
 9 represented by the confluent and direct resistance coefficients, are the linchpin for balancing the  
 10 branch-loop flow resistance and ensuring uniform exhaust for the ventilation system. The sectional  
 11 size of main and branch duct is determined by the common hydraulic calculation, based on the  
 12 farthest branch loop and the recommended velocity in duct. The confluent flow ratio at each  
 13 branch is pre-specified for the uniform exhaust concerned. Therefore, the crucial parameter for the  
 14 uniform exhaust design is the branch outlet height  $h$  of the flow-guide device.

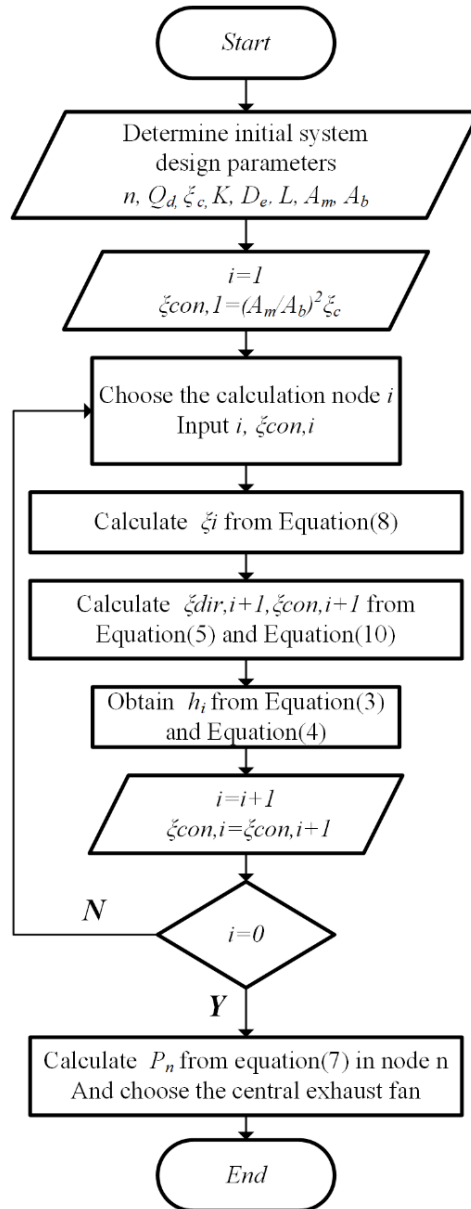
15 To fulfil the uniform exhaust, the resistance coefficients of the two adjacent devices should  
 16 satisfy

$$17 \quad \xi_{con,i} = \left(\frac{i-1}{i}\right)^2 (\xi_{con,i-1} + \xi_{i-1}) + \xi_{dir,i} \quad (10)$$

18 And for the first branch duct where the flow-guide device is not installed to ensure lower local  
 19 flow resistance, Eq.10 should be modified into

$$20 \quad \xi_{con,1} = \left(\frac{A_m}{A_b}\right)^2 \xi_c \quad (11)$$

21 Where the  $\xi_{con,1}$  is the virtually equivalent resistance coefficient of the first branch, donated by the  
 22 90°elbow connecting the branch#1 and the main duct, whose resistance coefficient is  $\xi_c$ .  
 23 Combining **Eqs. 3-11**, we can organize a calculating flowchart as the following **Fig.10**  
 24 to accomplish the parametric design of flow-guide devices for uniform exhaust and then determine  
 25 the pressure head requirement of the central exhaust fan in the ductwork. After the initial system  
 26 parameters were determined, we can attain  $\xi_{con,1}$  and  $\xi_1$  from **Eq.11** and **Eq.8**, which will be then  
 27 substituted into **Eq.10**. By jointly solving the **Eq.10** and **Eq.5**,  $\xi_{con,2}$  and  $\xi_{dir,2}$  can be calculated.  
 28 The  $\xi_{dir,2}$  can be plugged into **Eq.4** and solve the velocity ratio so that  $h_2$  can be determined by  
 29 **Eq.3**. The  $\xi_{con,2}$  will be then used for the next calculation node, repeating the above procedure.  
 30 After the iteration is completed, the distribution of  $h$ ,  $\xi_{con}$ , and  $\xi_{dir}$  can be all determined. The  
 31 pressure head of the central fan  $P_n$  can be subsequently known by **Eq.7** of node n.



1 **Fig.10** Calculating flowchart for the parametric design of the flow-guide device

2

3 **4 Real Application**

4 **4.1 Design results**

5 In order to validate the actual performance of the flow-guide device, a real-world application  
 6 was chosen referring to a real central exhaust system of a factory workshop with 30 heat and  
 7 contaminant sources in Shanghai. The initial information of the system is listed in **Table1**. The  
 8 total pressure loss coefficient of the elbow in branch #1 has been pre-tested under the designed  
 9 flowrate.

10

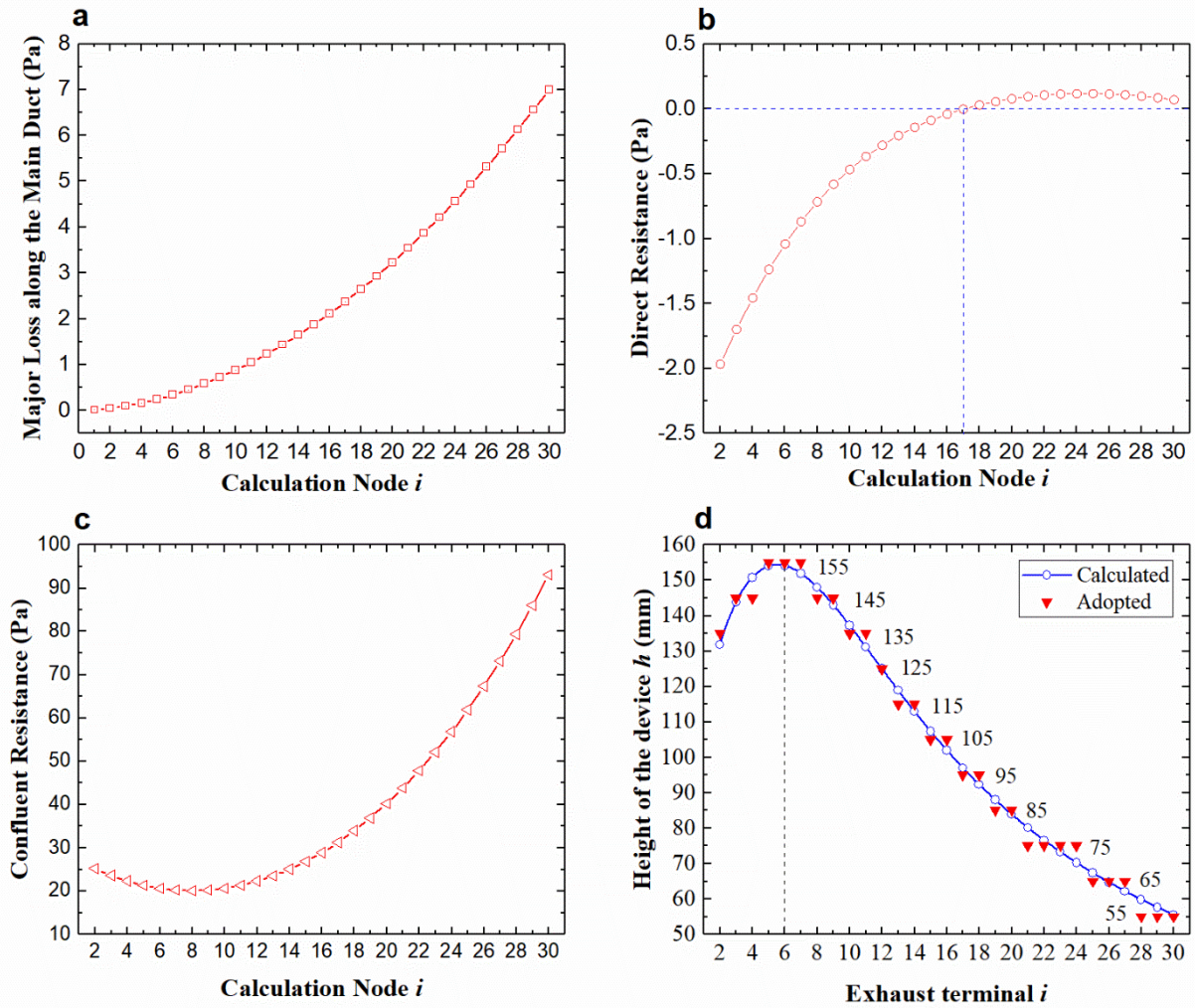
11 **Table1.** Initial information of the real-application system

1

Term	Terminal Numbers $n$	Branch Design Flowrate $Q_d(\text{m}^3/\text{h})$	Loss Coefficient of Elbow in Branch #1 $\xi_c$	Size of the Branch Duct (mm X mm)
Value	30	325	2.8	150 X150
Term	Roughness Degree $K(\text{mm})$	Length between Adjacent Terminals $L(\text{mm})$	Hydraulic Diameter of the Main Duct $De(\text{mm})$	Size of the Main Duct (mm X mm)
Value	0.15	3000	495	450 X 550

2

3 According to the parametric design procedure established in **Sec.3.2** , the required resistance  
4 values and the device height of each exhaust terminal were calculated. The major losses of the  
5 main duct is increasing with the increment of the total flowrate in main duct, as is shown in  
6 **Fig11.a**. Therefore, at the farthest terminal#1 with lowest main flowrate, the major losses is  
7 extremely small while it plays the dominant role at the nearest terminal away from the central fan.  
8 **Fig11.b** demonstrates the direct resistance distribution of each terminals. Opposite to the major  
9 losses along the main duct, the direct resistance shows negative value at terminals (#2-#17) and  
10 keeps relatively low positive value at the rest terminals. The negative feature is resulted from the  
11 low velocity ratio  $V_m/V_h$  (below 1) at far terminals, as is analysis in **Sec.2.4**. In this situation, the  
12 negative direct resistance help increase the driven force for the exhaust flow through far branches.  
13 The flow-guide device functions as some virtual booster fan in the main duct. These virtual fan  
14 can overcome the major losses of the main duct at the far terminals and thus present total negative  
15 loss along the main duct at the interval between terminals (#2-#8). As it is known in **Eq.10**, the  
16 difference value of the confluent resistances between adjacent devices functions to offset the total  
17 pressure loss along the main duct between these two branches. Therefore, the confluent resistance  
18 firstly decreases at the section with total negative loss and then increases, as is shown in **Fig11.c**.  
19 It reaches the lowest value at the middle terminal #8. Thus, contrary to our anticipation, we found  
20 that the peak value of the device height is not at the farthest terminal but in the middle. Then it  
21 declined by the trend of approximately linear relation. **Fig11.d** depicts the design results of the  
22 device height distribution and adopted values. As is studied in **Sec.2.4**, the resistance coefficients  
23 are not sensitized to the device height when the flow rate ratio is relatively low. Therefore, one  
24 single value of height may be acceptable for some adjacent devices with low flow rate ratios. Such  
25 simplification reduces the manufacturing cost. Therefore, eleven values of height are adopted in  
26 this real application system.



1 **Fig.11** Calculation results of design process: (a) The major losses along the main duct of each  
2 calculation node (b) The direct resistance of the flow-guide device in each calculation node (c)  
3 The confluent resistance of the flow-guide device in each calculation node (d) The device height  
4 distribution of exhaust terminals

5

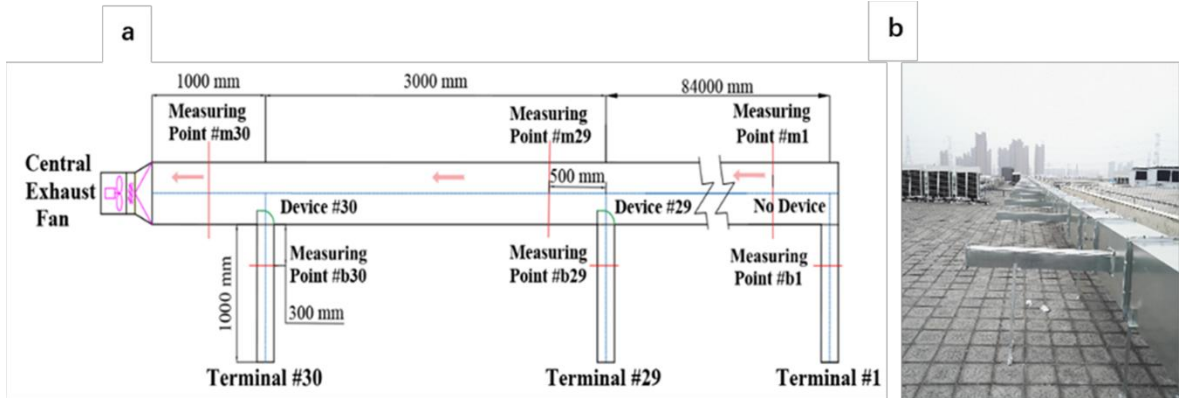
#### 6 4.2 Full-scale test

7 The 1:1 full-scale test was carried out according to the information listed in **Table 1**. As  
8 shown in **Fig12**. It consists of a central exhaust fan, a main duct, 30 branch exhaust terminals, the  
9 flow-guide devices and several measuring points. Ambient air instead of real polluted gas is  
10 chosen as the flow medium in the experiment. The rated airflow rate and pressure head of the  
11 central exhaust fan are  $12000\text{m}^3/\text{h}$  and  $300\text{Pa}$ . The sizes of these installed devices are chosen  
12 according to **Sec.4.1**.

13 The systems with and without the flow-guide devices were both tested. The airflow rate of each  
14 terminal, the static pressure distribution along the main duct and the energy consumption of the  
15 central fan were all measured. The static pressure along the main duct and the dynamic pressure in  
16 the branch duct were measured, as well as the energy consumption of the central fan. Three

1 repeated measurements were conducted to ensure the accuracy. **Table 3** shows the detailed  
 2 information of the measuring devices used in this test.

3



4 **Fig.12** Full-scale experiment system: (a) Schematic diagram of the test platform; (b) Field photo

5

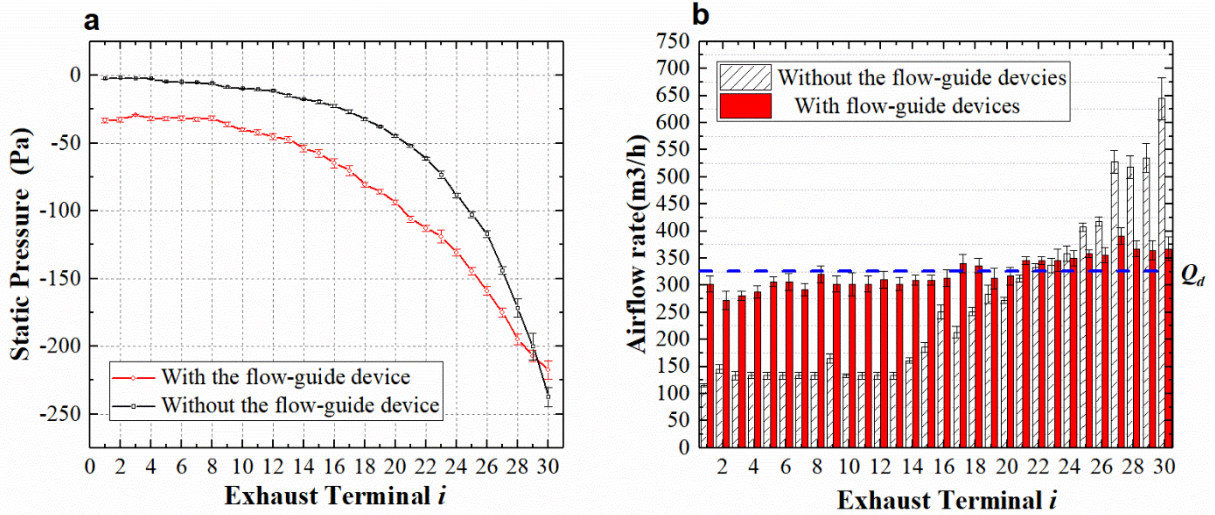
6 **Fig13** shows the static pressure distribution along the main duct and the airflow exhaust rate  
 7 of each terminal. Compared to the system without the flow-guide device, the exhaust rate  
 8 distribution was inclined to reach the average level, showing that the properly-designed  
 9 flow-guide device can basically realize uniform exhaust. The airflow discrepancy and exhaust  
 10 uneven degree are defined to evaluate the exhaust uniformity of the central air system, as follow:

11 
$$\Delta Q = Q_{max} - Q_{min} \quad (12)$$

12 
$$\beta = \frac{\sqrt{\sum(Q_i - Q_{ave})^2 / (n-1)}}{Q_{ave}} \quad (13)$$

13 The detailed calculation and measurement results are presented in **Table2**. The airflow discrepancy  
 14 is decreased by 80% and the uneven degree is reduced from 0.498 to 0.090. The exhausted airflow  
 15 rate of the farthest terminal greatly increases, reaching close to the design value. Thus, the  
 16 traditional problem of insufficient exhaust of the farthest terminal is solved by installing the  
 17 flow-guide device.

18 After applying the flow-guide devices, the resistance characteristic curve of the total system  
 19 is greatly changed and thus the system operating point was offset. Surprisingly the total rate of the  
 20 system increases from 7772 m<sup>3</sup>/h to 9717 m<sup>3</sup>/h. Meanwhile, the total pressure loss of the system is  
 21 decreased by 23.8% from 191.8 Pa to 146.2 Pa. Apparently, the total flow impedance of the  
 22 system declined with the flow-guide devices installed. Moreover, the test results showed that the  
 23 energy consumption of the central fan decreased from 11.12 kW to 10.73 kW.



1 **Fig.13** Test results of the systems with and without the flow-guide device: (a) Static pressure  
 2 distribution (b) Airflow rate distribution

3

4

**Table.2** Detailed results of the test

5

Term	$Q_{\max}$ (m <sup>3</sup> /h)	$Q_{\min}$ (m <sup>3</sup> /h)	$\Delta Q$ (m <sup>3</sup> /h)	$Q_{\text{tot}}$ (m <sup>3</sup> /h)	$\beta$	$\Delta P_{\text{sys}}$ (Pa)	E (kW)
Without devices	645	115	530	7772	0.498	191.8	11.12
With devices	391	272	119	9717	0.090	146.2	10.73
Changing Rate	39.4%	136.5%	77.5%	25.0%	81.9%	23.8%	3.5%

6

7

**Table.3** Detailed parameters of measurement apparatus

8

Term	Type	Range	Error	Accuracy
Hot-wire anemometer	TSI8385A	0-50 m/s	±3%	0.01m/s
Electronic micro-manometer	E0-1000Pa	0-1000Pa	±3%	1Pa
Clamp on power hitester	CM3286-01	0.05-632.5kw	±3%	0.01kw

9

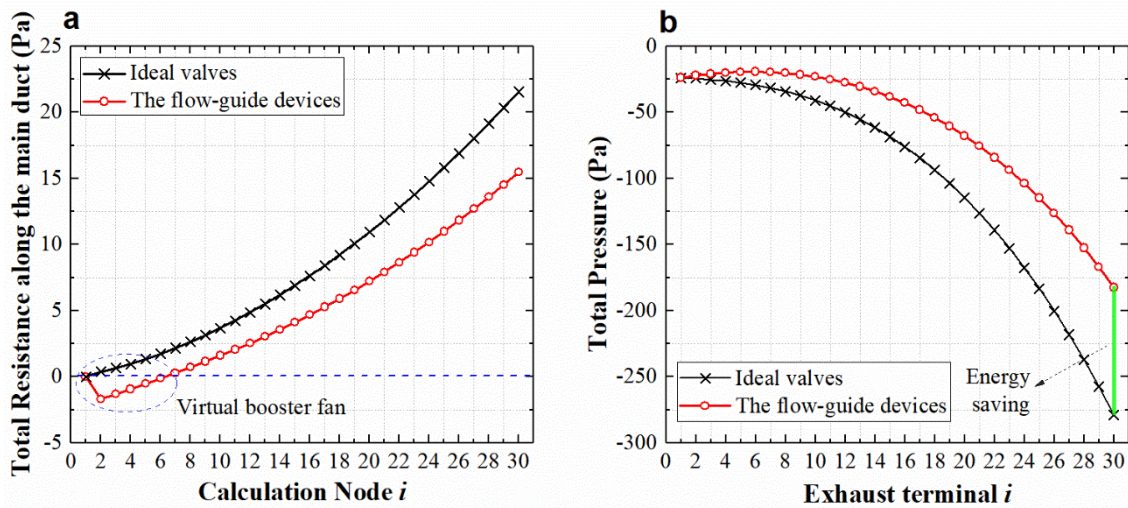
## 10 **5 Discussion**

11 The proposed novel design of flow-guide device in this paper could fulfill even exhaust by  
 12 means of properly designing the device height. Surprisingly, the confluence resistance can balance  
 13 the system well while the direct resistance at far terminals shows great negative value. The  
 14 accumulation of the negative direct resistance the devices bring could make a great difference.  
 15 Therefore, the new system could save the energy consumption of the central fan. Besides, the  
 16 traditional systems using dampers always need a TAB process after installation, while the system  
 17 balanced by the new flow-guide device does not need any adjusting process with propitiate

1 pre-design of the devices, which shows another superiority.

2 Assuming that the exhaust uniformity has already satisfied in system of **Sec.4** by ideal  
 3 valves or flow-guide devices, the flow resistance and total pressure distribution for these two  
 4 scenarios (with ideal valves versus flow-guide device) are further compared. **Fig14 (a)** shows the  
 5 resistance along the main duct of the two scenarios. The flow resistance of the ideal valve system  
 6 consists of the major losses of the main duct and direct resistance of the Tee-junction while the  
 7 device system transformed the latter one into that of flow-guide device. The flow-guide devices at  
 8 far terminals shows negative direct resistance and relatively lower resistance than the normal  
 9 Tee-junction at the close terminals. Therefore, the flow resistance along the main duct is smaller in  
 10 the device system than the ideal valve system. The section between terminal#1 and terminal #6  
 11 presents pressure gain instead of loss in the flow-guide device scenario. It acts as a virtual booster  
 12 fan that helps the exhaust in the main duct. **Fig14 (b)** shows the total pressure distribution along  
 13 the central duct. The device system shows a lower total pressure loss and thus a fan with lower  
 14 pressure head could be used. Approximately 35% total resistance reduction rate could be achieved  
 15 comparing with the ideal valve system.

16

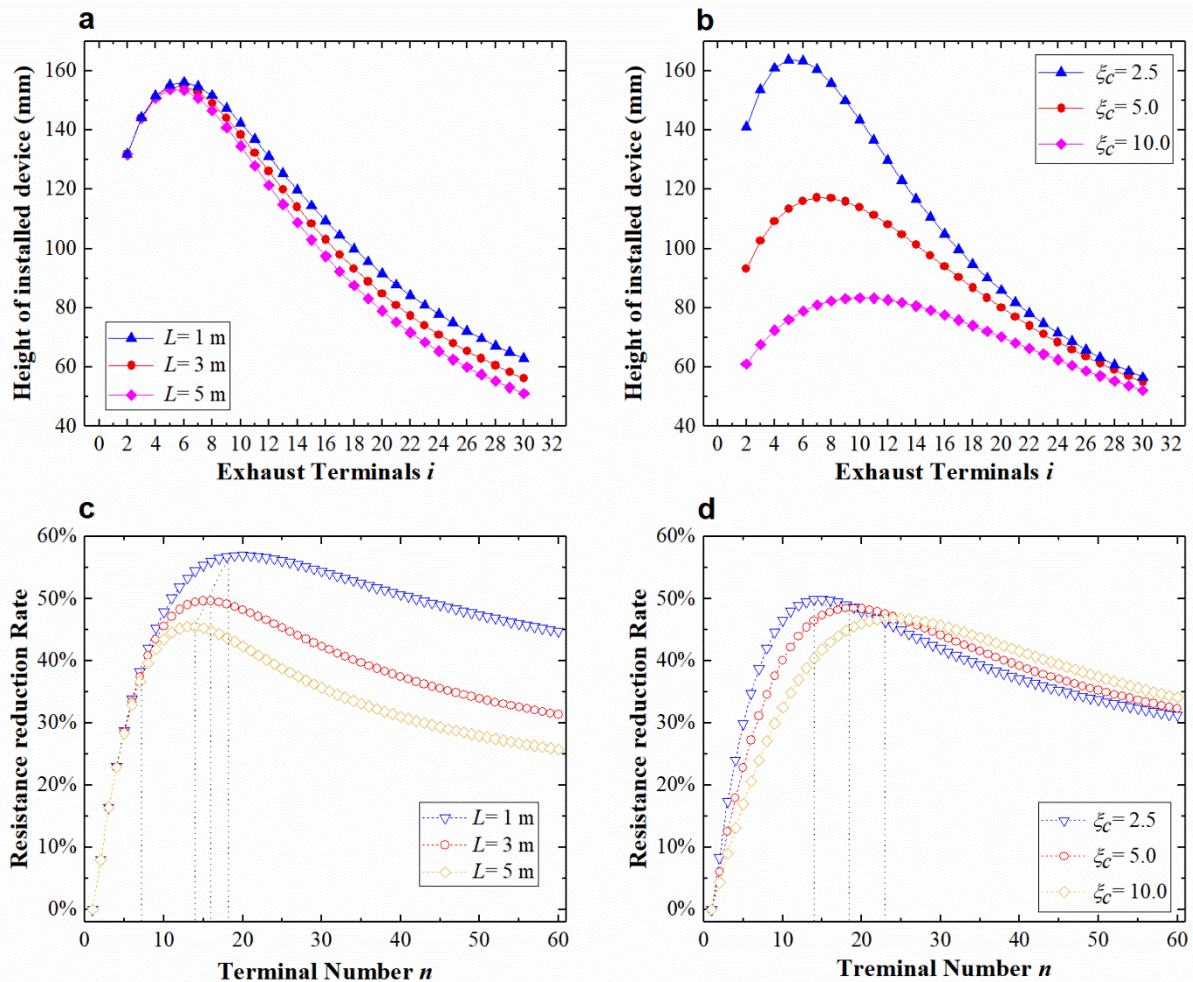


17 **Fig.14** Comparison between the systems balanced by valves and devices (a) Resistance along the  
 18 main duct (b) Total pressure distribution;

19

20 Take the system in **Sec.4** for example, the optimum height distribution of the devices are  
 21 mainly affected by the resistance coefficient of the elbow in branch#1  $\xi_c$  and the frictional  
 22 resistance of the main duct  $\xi_i$ . **Fig15 (a)** demonstrates the influence of the major losses along the  
 23 main duct upon the device height distribution. The curve of device height drops faster from the  
 24 peak with the larger major losses. While the height of the first few devices is almost the same as *L*  
 25 changes. **Fig15 (b)** depicts that the resistance coefficient  $\xi_c$  greatly affect the initial and peak value  
 26 of the device height. The two values decrease with  $\xi_c$  increasing. But the height of those terminals  
 27 close to the central fan is not sensitive to  $\xi_c$ .

1 Although the flow-guide device shows a good potential of resistance reduction, the energy  
 2 saving potential does not increase with the number of flow-guide device increasing, for the reason  
 3 that the flow-guide effect would become weakened as the flow ratio decreases. We found that the  
 4 resistance reduction rate would increase rapidly at the beginning and then reaches a peak value  
 5 with the increment of terminal numbers  $n$ . After that, it declines slowly with  $n$  increasing. The  
 6 major losses  $\xi_i$  and the resistance of the elbow in branch#1  $\xi_c$  are found to have significant impact  
 7 on the loss reduction rate. **Fig15.(c)** shows that larger major losses would lead to a smaller  
 8 reduction rate and the peak value. However, the loss reduction rate seems to have little relation  
 9 with the major resistance along the main duct when  $n$  is relatively small. **Fig15.(d)** tells that the  $\xi_c$   
 10 affects the value of terminal number that corresponding to the peak of the reduction rate. Before  
 11 the peak, the reduction rate decrease with  $\xi_c$  increasing. While the terminal number is large enough,  
 12  $\xi_c$  shows less impact.  
 13



14 **Fig.15** The device height distribution and resistance reduction rate comparing to the ideal valve  
 15 system: **(a)** Influence of the distance between adjacent branches  $L$  on the height distribution; **(b)**  
 16 Influence of the resistance coefficient  $\xi_c$  on the height distribution **(c)** Influence of  $L$  and Terminal  
 17 Number  $n$  on the resistance reduction rate; **(d)** Influence of  $\xi_c$  and terminal number  $n$  on the

1 resistance reduction rate;

2

### 3 **6 Conclusion**

4 A novel flow-guide device is developed for uniform exhaust in central exhaust ventilation  
5 system. This device is integrated in the converging Tee-junction with a partial-arc structure, which  
6 is added at the outlet of the branch that “guides” the branch flow to the main flow without distinct  
7 collision. Experimental studies and numerical simulations are both conducted to understand its  
8 resistance characteristics. It is found the new flow-guide device can function as a regulating  
9 damper through adjusting the structural parameter  $h$ . We further extend the work with only one  
10 branch duct into a central exhaust system with multiple terminals. The ductwork hydraulic model  
11 is established according to the Bernoulli’s Law and flow continuity. Combining with the  
12 regression formulas of the device resistance coefficients, a parameterized design method is built  
13 up to determinate the structural parameter of the devices applied in each terminal. A real-world  
14 application referring to a factory workshop with 30 heat and contaminant sources in Shanghai is  
15 adopted to explore the performance of the devices. Based on the current study, several conclusions  
16 could be summed up in this paper as below:

- 17 (1) The resistance characteristics of the flow-guide device changes with the flow rate ratio of  
18 flow rate  $Q_b/Q_m$  and the sectional area ratio  $A_b/A_m$ . The confluent resistance coefficient  
19 increases with the increment of  $Q_b/Q_m$  and decreases with increment of  $A_b/A_m$ . While the  
20 direct resistance coefficient shows the opposite feature.
- 21 (2) When the velocity ratio  $V_m/V_h$  is below 1 as the device narrows down the branch flow  
22 outlet, the direct resistance presents negative value due to the high-velocity airflow being  
23 injected into the main duct. In central exhaust system, the negative direct resistance of  
24 the flow-guide devices help increase the driven force for the exhaust flow through far  
25 branches.
- 26 (3) The flow-guide device can act as a regulating valve through adjusting the height  $h$  of the  
27 device to realize uniform exhaust that meets the engineering requirements. In the  
28 real-world application, the exhaust ventilation rates for all terminals got close to the  
29 design value after applying the flow-guide devices. Except for improving the exhaust  
30 uniformity, the total airflow rate of the system increased by 25% while the total flow  
31 resistance of the system decreased by 23.8%, which showed that the flow impedance of  
32 the system declined after the flow-guide devices installed.
- 33 (4) Comparing to the system balanced by ideal valve, approximately 35% total resistance  
34 reduction rate could be achieved by the flow-guide device. Besides, system using normal  
35 regulating dampers need a TAB process after installation, while the system balanced by  
36 the flow-guide device with proper pre-design does not need any commissioning or  
37 regulating process.
- 38 (5) With the terminal number increasing, the resistance reduction rate would firstly increase

1 rapidly at the beginning. After reaching a peak value, it declines slowly and the major  
2 losses of the main duct is found to have significant impact.

### 3 **Acknowledgements**

4 This research has been supported by the China National Key R&D Program during the 13th  
5 Five-year Plan Period (Grant No.2018YFC0705300). Support from the National Natural Science  
6 Foundation of China under grant No.51578387 and No.51778440 in this study are also gratefully  
7 acknowledged.

### 8 **References**

- 9 [1] Jiangyan Ma, Xin Zhang, et al., *Analyses of the Improvement of Subway Station Thermal*  
10 *Environment in Northern Severe Cold Regions*. Build Environ, 2018. **143**: p. 579-590. DOI:  
11 10.1016/j.buildenv.2018.07.039
- 12 [2] Changsheng Cao, Jun Gao, et al., *Ventilation Strategy for Random Pollutant Releasing from*  
13 *Rubber Vulcanization Process*. Indoor Built Environ., 2017. **26**(2): p. 248-255. DOI:  
14 10.1177/1420326x16683537
- 15 [3] Yanqiu Huang, Yi Wang, et al., *Reduced-Scale Experimental Investigation on Ventilation*  
16 *Performance of a Local Exhaust Hood in an Industrial Plant*. Build Environ, 2015. **85**: p.  
17 94-103. DOI: 10.1016/j.buildenv.2014.11.038
- 18 [4] Ashrae Standard Committee, *Ashrae Handbook: Fundamentals 2013*. ASHRAE, 2013.
- 19 [5] S.C. Sugarman, *Testing and Balancing Hvac Air and Water Systems*. Fairmont Press, 2006.
- 20 [6] Hotupan Anca Domnita Florin, Popovici Tudor, *Total Air Pressure Loss Calculation in*  
21 *Ventilation Duct Systems Using the Equal Friction Method* Journal of Applied Engineering  
22 Sciences, 2012. **2**(15)(1): p. 25-30.
- 23 [7] Ping Yin, *Improved Method of Multiple-Branch Duct System Calculation on the Static Regain*  
24 *Method*. Hv & Ac, 2001. **31**(2): p. 18-22. (in Chinese).
- 25 [8] H.F. Behls R.J. Tsal, R. Mangel, *T-Method Duct Design. I: Optimization Theory*., ASHRAE  
26 Trans. 94, 1988: p. 90-111.
- 27 [9] Huan-Ruei Shiu, Feng-Chu Ou, and Sih-Li Chen, *Optimization Design of Exhaust Duct*  
28 *System in Semiconductor Factory Using Dynamic Programming Method*. Build Environ, 2003.  
29 **38**(4): p. 533-542. DOI: 10.1016/S0360-1323(02)00181-6
- 30 [10] E. Guffey, Spann, G., *Experimental Investigation of Power Loss Coefficients and Static*  
31 *Pressure Ratios in an Industrial Exhaust Ventilation System*. American Industrial Association  
32 Journal, 1999. **60**(3): p. 367-376. DOI: 10.1080/00028899908984455
- 33 [11] Wen Liang Chen, Mao Ching Lin, et al., *Feedback Simulation and Correction of Duct Design*  
34 *for Acidity Exhaust System in a Semiconductor Factory*. Journal of the Chinese Society of  
35 Mechanical Engineers, 2001. **22**. DOI: 140.112.114.62/handle/246246/86518
- 36 [12] Wen Liang Chen and Ya Mei Chiang. *An Integrated System Simulation and Correction*  
37 *Process for Duct Design in the Industrial Building*. in *Network of Ergonomics Societies*  
38 *Conference*. 2012.
- 39 [13] Roger Legg, *Chapter 16 - Balancing Fluid Flow Systems*, in *Air Conditioning System Design*.  
40 2017, Butterworth-Heinemann. p. 319-342.
- 41 [14] Steven Guffey, *A Goal Method and a Target Method for Balancing Exhaust Ventilation Duct*  
42 *Systems with Dampers*. J Occup Environ Hyg, 2007. **4**(3): p. 224-235. DOI:  
43 10.1080/15459620601177503

- 1 [15] Michael Dodrill and Steven E. Guffey, *Experimental Validation of a Target Method for*  
2 *Balancing Exhaust Ventilation Duct Systems with Dampers*. J Occup Environ Hyg, 2008.  
3 **5**(11): p. 689-701. DOI: 10.1080/15459620802374677
- 4 [16] Steven E. Guffey, *Air-Flow Redistribution in Exhaust Ventilation Systems Using Dampers and*  
5 *Static Pressure Ratios*. Applied Occupational and Environmental Hygiene 1993. **8**(3): p.  
6 168-174. DOI: 10.1080/1047322X.1993.10389188
- 7 [17] Huei-Jiunn Chen, David W. P. Wang, and Sih-Li Chen, *Balancing Adjustment of Exhaust Duct*  
8 *System Using Feedback Simulation Method*. Appl Therm Eng, 2006. **26**(5-6): p. 463-470. DOI:  
9 10.1016/j.applthermaleng.2005.08.001
- 10 [18] Federico Pedranzini, Luigi P. M. Colombo, and Cesare M. Joppolo, *A Non-Iterative Method*  
11 *for Testing, Adjusting and Balancing (Tab) Air Ducts Systems: Theory, Practical Procedure*  
12 *and Validation*. Energy Build., 2013. **65**: p. 322-330. DOI: 10.1016/j.enbuild.2013.06.017
- 13 [19] Haoran Chen, Wenjian Cai, and Can Chen, *Model-Based Method for Testing, Adjusting and*  
14 *Balancing of Hvac Duct System*. Energy Build., 2016. **126**: p. 498-507. DOI:  
15 10.1016/j.enbuild.2016.05.037
- 16 [20] Haoran Chen, Wenjian Cai, and Can Chen, *Fan-Independent Air Balancing Method Based on*  
17 *Computation Model of Air Duct System*. Build Environ, 2016. **105**: p. 295-306. DOI:  
18 10.1016/j.buildenv.2016.06.008
- 19 [21] Shan Hu, Da Yan, et al., *A Survey on Energy Consumption and Energy Usage Behavior of*  
20 *Households and Residential Building in Urban China*. Energy & Buildings, 2017. **148**.
- 21 [22] Tsinghua Building Energy Research Center, *Annual Report on China, Building Energy*  
22 *Efficiency*. China architecture and building press. Beijing, China, 2014. (in Chinese).
- 23 [23] G. H. Gan and S. B. Riffat, *Numerical Determination of Energy Losses at Duct Junctions*.  
24 Appl Energ, 2000. **67**(3): p. 331-340. DOI: 10.1016/S0306-2619(00)00026-X
- 25 [24] Bastian Schmandt and Heinz Herwig, *The Head Change Coefficient for Branched Flows: Why*  
26 *“Losses” Due to Junctions Can Be Negative*. Int J Heat Fluid Fl, 2015. **54**: p. 268-275. DOI:  
27 10.1016/j.ijheatfluidflow.2015.06.004
- 28 [25] Xin Li and Shaoping Wang, *Flow Field and Pressure Loss Analysis of Junction and Its*  
29 *Structure Optimization of Aircraft Hydraulic Pipe System*. Chinese Journal of Aeronautics,  
30 2013. **26**(4): p. 1080-1092. DOI: 10.1016/j.cja.2013.04.004
- 31 [26] Ran Gao, Kaikai Liu, et al., *Biomimetic Duct Tee for Reducing the Local Resistance of a*  
32 *Ventilation and Air-Conditioning System*. Build Environ, 2018. **129**: p. 130-141. DOI:  
33 10.1016/j.buildenv.2017.11.023
- 34 [27] Ran Gao, Zhiyu Fang, et al., *A Novel Low-Resistance Tee of Ventilation and Air Conditioning*  
35 *Duct Based on Energy Dissipation Control*. Appl Therm Eng, 2017. **132**. DOI:  
36 10.1016/j.applthermaleng.2017.12.107
- 37 [28] Ran Gao, Kaikai Liu, et al., *Study of the Shape Optimization of a Tee Guide Vane in a*  
38 *Ventilation and Air-Conditioning Duct*. Build Environ, 2018. **132**: p. 345-356. DOI:  
39 10.1016/j.buildenv.2018.02.006
- 40 [29] Yantao Yin, Kai Chen, et al., *Mean Pressure Distributions on the Vanes and Flow Loss in the*  
41 *Branch in a T Pipe Junction with Different Angles*. Energy Procedia, 2017. **105**: p. 3239-3244.  
42 DOI: 10.1016/j.egypro.2017.03.718
- 43 [30] J. T. Haskew and M. A. R. Sharif, *Performance Evaluation of Vaned Pipe Bends in Turbulent*  
44 *Flow of Liquid Propellants*. Applied Mathematical Modelling, 1997. **21**(1): p. 48-62. DOI:

- 1 10.1016/s0307-904x(96)00121-7
- 2 [31] Tao Sun, Yi Zhang, and Zhongyi Wang, *Research on Flow in 90° Curved Duct with Round*
- 3 *Section*. Physics Procedia, 2012. **24**(Part A): p. 692-699. DOI: 10.1016/j.phpro.2012.02.102
- 4 [32] P. P. Modi and S. Jayanti, *Pressure Losses and Flow Maldistribution in Ducts with Sharp*
- 5 *Bends*. Chemical Engineering Research and Design, 2004. **82**(A3): p. 321-331. DOI:
- 6 10.1205/026387604322870435
- 7 [33] Mitsukiyo Murakami and Yukimaru Shimizu, *Hydraulic Losses and Flow Patterns in Pipes*
- 8 *with Two Bends Combined : Effects of Bend Curvature and Wall Roughness*. Jsme
- 9 *International Journal*, 2008. **20**(147): p. 1136-1144.
- 10 [34] Ran Gao, Zhiyu Fanga, et al., *Numerical Simulation and Experimental Study of the Drag*
- 11 *Reduction of 90 Elbows for Ventilation and Air Conditioning Tubes in an Arc Form*. Procedia
- 12 *Engineering*, 2017. **205**(2017): p. 3978-3985. DOI: 10.1016/j.proeng.2017.09.859
- 13 [35] Ran Gao, Zhiyu Fang, et al., *Numerical Simulation and Experimental Study on Resistance*
- 14 *Reduction Optimization of the Cambered Surface of Elbows under Adjacent Influence*.
- 15 *Procedia Engineering*, 2017. **205**(2017): p. 3985-3992. DOI: 10.1016/j.proeng.2017.09.864
- 16 [36] N. P. Costa, R. Maia, et al., *Edge Effects on the Flow Characteristics in a 90 Deg Tee Junction*.
- 17 *Journal of Fluids Engineering*, 2006. **128**(6): p. 1204-1217. DOI: 10.1115/1.2354524
- 18 [37] Kenji Oka, Takahito Nozaki, and Hidesato Ito, *Energy Losses Due to Combination of Flow at*
- 19 *Tees*. Jsme International Journal, 2008. **39**(3): p. 489-498. DOI: 10.1299/jsmeb.39.489
- 20 [38] Blaisdell F W and Manson P W, *Energy Loss at Pipe Junctions*. J.Irrig. and Drainage Div.,
- 21 ASCE, 1967. **93**: p. 59-78.
- 22 [39] Miller D S, *Internal Flow System*. BHRA(information Services)Cranfield, 1990.
- 23 [40] Idelchik I E, *Handbook of Hydraulic Resistance:Coefficient of Local Resistance and of*
- 24 *Friction*. Israel Program for Scientific Translations, 1966. DOI: 10.1115/1.3264907
- 25 [41] Serre M, Odgaard A J, and Elder R A, *Energy Loss at Combining Pipe Junction*. Journal of
- 26 *Hydraulic Engineering*, 1995. **120**(7): p. 808-830. DOI:
- 27 10.1061/(ASCE)0733-9429(1994)120:7(808)
- 28 [42] Riffat Sb Gan G, *K-Factors for Hvac Ducts — Numerical and Experimental Determination*.
- 29 *Building Services Engineering Research and Technology*, 1995. **16**(3): p. 133-139. DOI:
- 30 10.1177/014362449501600303
- 31 [43] Zengji Cai and Tianyu Long, *Fluid Mechanics: Pumps and Fans(Fifth Edition)*. China
- 32 *Architecture & Building Press*, 2009. (in Chinese).
- 33